01 Nov 1993

An Integrated Surface and Borehole Seismic Case Study: Fort St. John Graben Area, Alberta, Canada

Ronald C. Hinds

Richard Kuzmiski

Neil Lennart Anderson
Missouri University of Science and Technology, nanders@mst.edu

Barry R. Richards

Recommended Citation

R. C. Hinds et al., "An Integrated Surface and Borehole Seismic Case Study: Fort St. John Graben Area, Alberta, Canada," *Geophysics*, vol. 58, no. 11, pp. 1662-1675, Society of Exploration Geophysicists, Nov 1993.
The definitive version is available at https://doi.org/10.1190/1.1443382

GEOPHYSICS, VOL. 58, NO. 11 (NOVEMBER 1993); P. 1662–1675, 15 FIGS.

An integrated surface and borehole seismic case study: Fort St. John Graben area, Alberta, Canada

Ronald C. Hinds*, Richard Kuzmiski‡, Neil L. Anderson**, and Barry R. Richards§

ABSTRACT

The deltaic sandstones of the basal Kiskatinaw Formation (Stoddard Group, upper Mississippian) were preferentially deposited within structural lows in a regime characterized by faulting and structural subsidence. In the Fort St. John Graben area, northwest Alberta, Canada, these sandstone facies can form reservoirs where they are laterally sealed against the flanks of upthrown fault blocks. Exploration for basal Kiskatinaw reservoirs generally entails the acquisition and interpretation of surface seismic data prior to drilling. These data are used to map the grabens in which these sandstones were deposited, and the horst blocks which act as lateral seals. Subsequent to drilling, vertical seismic profile (VSP) surveys can be run. These data supplement the surface seismic and well log control in that:

1) VSP data can be directly correlated to surface seismic data. As a result, the surface seismic control can be accurately tied to the subsurface geology;
2) Multiples, identified on VSP data, can be deconvolved out of the surface seismic data; and
3) The subsurface, in the vicinity of the borehole, is more clearly resolved on the VSP data than on surface seismic control.

On the Fort St. John Graben data set incorporated into this paper, faults which are not well resolved on the surface seismic data, are better delineated on VSP data. The interpretive processing of these data illustrate the use of the seismic profiling technique in the search for hydrocarbons in structurally complex areas.

INTRODUCTION

On the basis of conventional surface seismic data, an exploratory well (9-24-82-11W6M) was drilled into the basal Kiskatinaw Formation (Stoddard Group, upper Mississippian; Figure 1) on the downthrown side of a fault block in the Fort St. John Graben area, Peace River Embayment (Figures 2 and 3). The expectation was that gas-prone sandstones of the basal Kiskatinaw would be laterally truncated and sealed against shales of the Golata Formation. Contrary to expectations, the well encountered unproductive, shaly-sandstone tidal-flat facies in the basal Kiskatinaw and commercial gas-bearing zone in the upper Kiskatinaw, and is now shut-in. To obtain a higher resolution image of the subsurface in the vicinity of the well bore, and to evaluate the proximity of any fault features that might not have been resolved on the surface seismic data, three VSP (vertical seismic profile) surveys were run. These seismic profiles were used in conjunction with surface seismic coverage to cooperatively image the fault systems in the area and to elucidate the seismic signature of the unexpected upper Kiskatinaw reservoir.

This paper is a case history of the Fort St. John Graben 9-24 well. We include an overview of the stratigraphy (Figure 1) and the geologic history of the Lower Carboniferous in the study area. We describe the acquisition and interpretive processing of the VSP data and present an integrated interpretation of the well log, surface seismic, and seismic profile data.

LOWER CARBONIFEROUS: FORT ST. JOHN GRABEN AREA

Within the Carboniferous succession in the Fort St. John Graben area (Figures 1, 2, and 3), four principal episodes of block faulting have been recognized (Richards, 1989, 1990):

Manuscript received by the Editor December 16, 1991, revised manuscript received February 28, 1993.
*Department of Geology, University of Pretoria, South Africa 0002.
‡Computalog, 800, 600-6th Avenue SW, Calgary, Alberta T2P 0S5.
**Kansas Geological Survey, University of Kansas, 1930 Constant Ave., Campus West, Lawrence, KS 66047.
§Institute of Sedimentary and Petroleum Geology, 3303-33rd St. NW, Calgary, Alberta, T2L 2A7.

1) After deposition of the latest Devonian to earliest Carboniferous deposits of the Exshaw Formation, but prior to the deposition of the Banff Formation;
2) During deposition of the lower Banff;
3) During the deposition of the Golata and Kiskatinaw formations; and
4) After deposition of the Taylor Flat Formation but prior to that of the Permian Ishbel Group (Richards et al., in press).

Marked regional subsidence accompanied the second and third phases of blockfaulting, whereas subaerial erosion and local uplift accompanied the first and last phases. The Golata, Kiskatinaw, and Taylor Flat formations were deposited during the third episode of blockfaulting. The Golata consists of fissile dark grey mudstone, siltstone, and shale (Barclay, 1988). This pro-delta sequence can serve as a reservoir seal in those places where, as a result of faulting, it is juxtaposed against the sandstones of the basal Kiskatinaw.

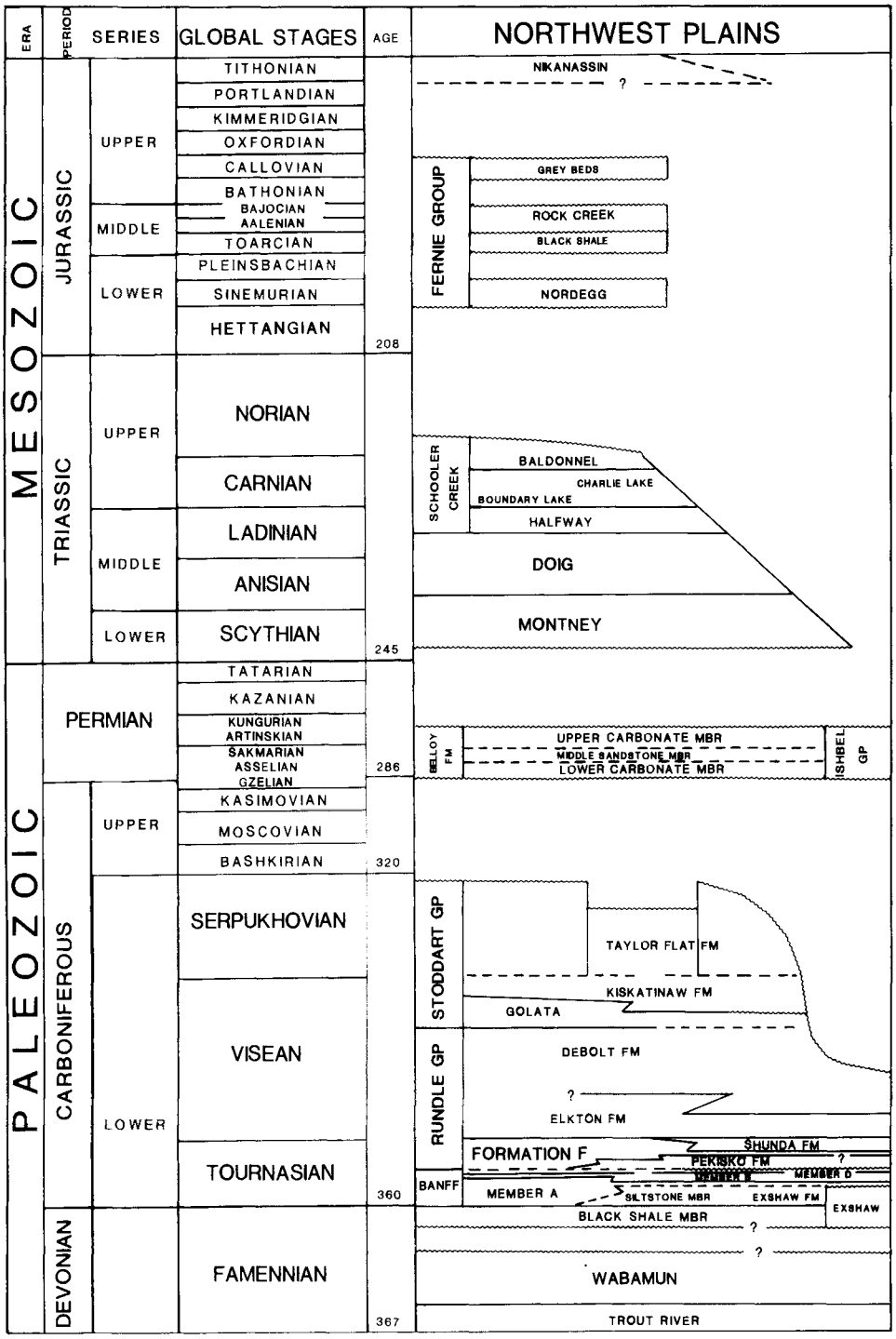

FIG. 1. Upper Paleozoic/lower Mesozoic stratigraphy of the Peace River Embayment area, Western Canada Sedimentary Basin (after Richards, 1989).

The Kiskatinaw consists predominantly of sandstone with minor quantities of fine grained siliciclastics, limestones, dolostones, and coals. At least eight depositional cycles subdivide the formation, but three main depositional cycles are referred to informally as the basal, middle, and upper Kiskatinaw. The channel fills of the basal Kiskatinaw (Barclay, 1988) were the target of the 9-24 well. The hypothesis was that thick sections of basal Kiskatinaw would be preferentially deposited in the structural lows on the downthrown side of early Kiskatinaw faults. The basal Kiskatinaw encountered by the 9-24 well was not of reservoir quality; however, the sandstones of the upper Kiskatinaw contain commercial gas.

ORIGINAL INTERPRETATION AND WELL RESULTS

One of the surface seismic lines used in the initial evaluation of the Fort St. John Graben area is shown as Figure 4. These split-spread, 96 trace data were acquired using a patterned dynamite source (3 × 3 kg at 15 m) and DFS IV recording equipment [12/18-124 Hz filter; notch (60 Hz) filter out]. The groups consisted of nine inline 14-Hz L25D geophones spaced at 6.1 m. The geophone group, shot, CMP, and near offset intervals were 67.1, 134.1, 33.5, and 201.2 m, respectively.

The seismic section (normal polarity display; Figure 4) was migrated using a prestack partial migration scheme that consisted of applying a common-offset domain, dip-moveout (DMO) correction (Hale, 1984) to the prestack data. Updated velocities were then determined using DMO-corrected CMP gathers. Closely spaced velocity analyses were performed since the stacking velocities changed rapidly along the line. This prestack processing was followed by poststack phase-shift migration (Gazdag, 1978; Gazdag and Squazzero, 1984).

The surface seismic data were used to elucidate the structural setting at the Kiskatinaw level. The interpreted events on the seismic line are the Nordegg, Halfway/Doig, Belloy, basal Kiskatinaw, and Debolt (Figures 1 and 4). The 9-24-82-11W6M well was located approximately 200 m east of the seismic line and has been projected as shown. Note that 9-24, as projected, is on a downthrown fault block relative to 2-25-82-11W6M and 7-36-82-11W6M (Figure 4).

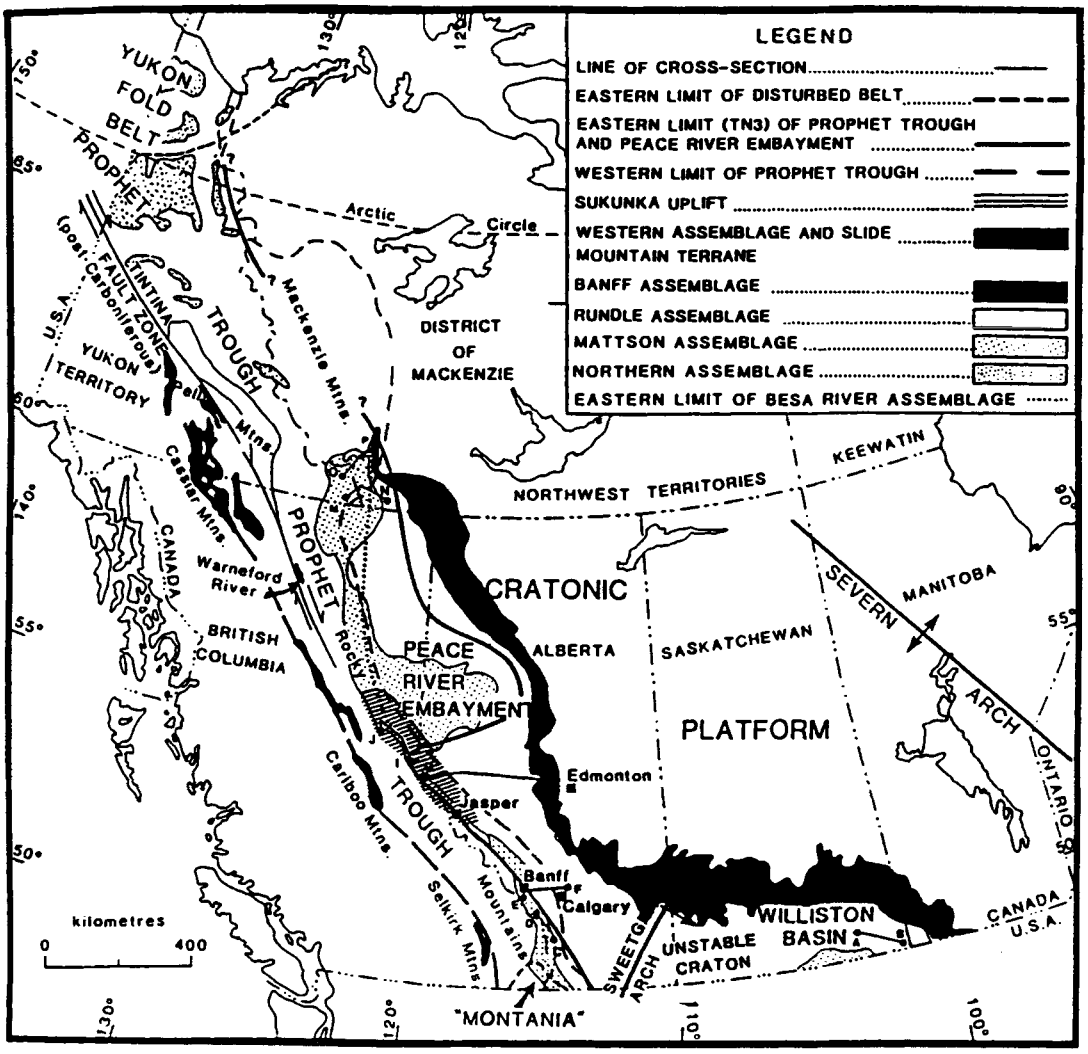

FIG. 2. Map of western Canada showing the Peace River Embayment area (after Richards, 1989). The Fort St. John area is located in the northern part of the Peace River Embayment area.

The 2-25 well (Figure 3) encountered approximately 25 m of relatively clean, wet basal Kiskatinaw sandstone and was abandoned. The 7-36 well penetrated 35 m of basal Kiskatinaw sandstone that tested gas plus salt water and is currently classified as a shut-in gas well. Well 9-24 was drilled in the expectation that basal Kiskatinaw gas would be stratigraphically entrapped against the flank of the upthrown fault block; however the basal Kiskatinaw proved to be shaly sandstone and not of reservoir quality. The 9-24 well was shut-in as an upper Kiskatinaw gas well.

VSP ACQUISITION

Three VSP surveys were run at the 9-24 well site (one near-offset and two far off-set sources). There were several primary objectives:

1) To provide confident surface seismic ties to:
   a) The upper Kiskatinaw reservoir
   b) The basal Kiskatinaw, and
   c) The Debolt;
2) To determine if multiple reflections were a significant problem at the Kiskatinaw level and to design an effective deconvolution filter;
3) To map the lateral extent of the upper Kiskatinaw reservoir and the basal Kiskatinaw shaly sandstone in the direction of the far-offset VSPs;
4) To provide a higher resolution seismic image of the Debolt faults in the vicinity of the 9-24 well.

The near-offset source was located 149 m from 9-24 and in the direction of 2-25; far-offset 1 (LO1), also located in the direction of 2-25, was 700 m from 9-24; far-offset 2 (LO2) was situated 741 m east of 9-24. Two Vibroseis units operated in tandem series at each offset using a 12 s input sweep of 10-90 Hz. The recording length was 15 s resulting in a 3 s cross-correlated output. On average, six sweeps were summed at each geophone sonde location. The total depth of 9-24 was 2126 m below KB (KB at 644 m asl). All three offset sources were at 639 m asl. Data were recorded at a sampling rate of 1 ms using an MDS-10 unit. The recording filter OUT/250 was designed to prevent aliasing.

The triaxial sonde depth spacing was 20 m (from a depth of 2030 m up to 350 m). As a precautionary measure, calibration records were acquired at several depths as the sonde was lowered down the borehole and again during the production runs to detect possible depth errors or cable stretch.

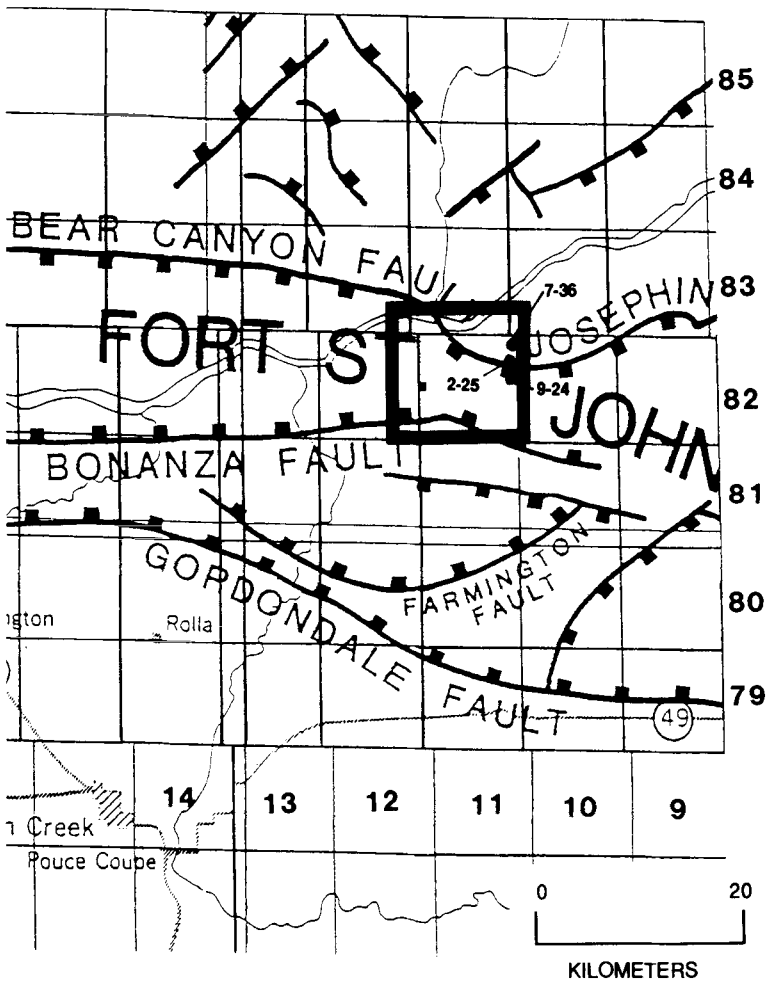

FIG. 3. Detailed map of the Fort St. John study area, northwest (after Richards et al., in press). The study area is centered on Township 82, Range 11 West of the 6th Meridian.

NEAR-OFFSET VSP INTERPRETIVE PROCESSING

During the processing of the near-offset VSP data a series of interpretive processing panels (IPPs) were generated. These panels display the following interpretive processing steps:

1) Upgoing and downgoing *P*-wave separation;
2) Deconvolution of the separated upgoing *P*-waves; and
3) Inside and outside corridor stacks of both the nondeconvolved and deconvolved upgoing waves.

Throughout the paper, the abbreviations FRT, −TT time and +TT time (Hinds et al., 1989) are used repeatedly. FRT is the abbreviation for field recorded time, the term used to describe the time-depth display of the raw field records. The terms −TT and +TT refer to specific data configurations. −TT is used in reference to displays on which the first breaks and downgoing waves are aligned and bulk shifted. On these displays the first-break traveltime has been subtracted from each trace, and the aligned traces have been bulk-shifted to an arbitrary time-datum (usually to 100 or 200 ms). +TT is used in reference to displays on which the first break time of each trace has been added to that trace (plus possible NMO corrections). On the +TT displays the upgoing waves are aligned and should be in pseudo two-way traveltime. Except as noted, the VSP displays are normal polarity.

P-wave separation; near-offset VSP

The separation of upgoing and downgoing *P*-waves [vertical (Z) geophone data] is depicted in the wavefield separation interpretive processing panel or IPP (Hinds et al., 1989) of Figure 5.

Panel 1 displays the raw Z data after trace normalization. The upgoing *P*-wave events are difficult to discern until these data are gain adjusted (panel 2). On these panels, the tube wave is visible below 0.9 s as a high-frequency, downgoing wave train with a velocity of about 1435 m/s. The tube wave reflects from the bottom of the borehole (between 1.4 and 1.8 s on panel 1) and travels back up the borehole.

Several upgoing primary events and multiple reflections can be identified on panel 2. Consider for examples, Spirit River and Nordegg events. Each of these events is followed by a trailing surface-generated multiple with a lag time of about 110 ms. This multiple pattern (both upgoing and downgoing waves) is highlighted in panel 2 of Figure 5.

In panel 3 (Figure 5), the combined wavefields are displayed such that the first breaks and downgoing multiple events are horizontally aligned. An 11-point median filter was used to remove the upgoing *P*-waves; the output separated and scaled downgoing waves are displayed in panel 4. In the following step, the downgoing *P*-wave data of panel 4 were subtracted from the combined wavefield to yield the output upgoing wavefield (panel 5). Note that the residual tube wave is visible in the separated upgoing wavefield (panel 5).

The upgoing waves before and after the application of a three-point median filter are shown in panels 6 and 7, respectively. In panel 7, the Spirit River multiple (highlighted in panel 2) is observed as high-amplitude events that lie directly below the Spirit River primary and can be interpreted for several cycles (from .65 to 1.0 s). This multiple is not observed at sonde depths below the top of the Spirit River (at 730 m).

Deconvolution; near-offset VSP

On VSP data, the initial downgoing pulse (except in the case of head wave contamination) is the primary downgoing *P*-wave; any later arriving, downgoing events are multiples (apart from downgoing shear or converted waves). Ideally, multiples can be effectively filtered using a deconvolution operator derived from an analysis of the downgoing wave train (Hardage, 1985; Hinds et al., 1989). Deconvolution also increases the dominant frequency of data, allowing for better vertical resolution.

The deconvolution IPP (Figure 6) enables the interpreter to monitor the deconvolution process. The incorporated panels reveal information (about multiples) that was difficult to determine from the wavefield separation IPP (Figure 5) alone. The first two panels (Figure 6) are the nonmedian and median-filtered, nondeconvolved upgoing wavefields, respectively. Panel 3 is the gain-adjusted downgoing wavefield. Panels 4 and 5 are the nondeconvolved and deconvolved, upgoing wavefields, respectively.

The last two panels (6 and 7) are the deconvolved, upgoing, nonmedian, and median filtered data, respectively. A comparison of panels 2 and 7 (Figure 6), shows that deconvolution has effectively attenuated multiple reflections. The Spirit River multiple wave train from 0.65 s to 1.0 s (panel 2), for example, has negligible amplitude on panel 7. Note also that deconvolution has decreased the dominant wavelength of the data, allowing for better resolution at the Kiskatinaw level.

Inside and outside corridor stack; near-offset VSP

Multiple contamination can also be analyzed on inside and outside corridor stacks. Inside corridor stacks of nondeconvolved data contain both primaries and multiples. Nondeconvolved outside corridor stacks are predominated by primary events (except in the case of severe head-wave contamination). Ideally, deconvolved inside and outside corridor stacks will contain primary events only.

Nondeconvolved, inside and outside corridor stacks and associated displays are presented in Figure 7. A comparison of the inside and outside corridor stacks (panels 4 and 9, respectively) illustrates the use of these displays. For example, the Spirit River multiple (between 0.65 and 1.0 s) is present on the inside corridor stack and absent on the outside corridor stack. Note also, that basal Kiskatinaw and Golata events can be resolved on the outside corridor stack; on the inside corridor stack these reflections are masked by a high-amplitude multiple.

If deconvolution is successful, the deconvolved, inside and outside corridor stacks (panels 4 and 9; Figure 8) should be similar. At the zone of interest, just above 1.3 s, the Golata and basal Kiskatinaw events are similar (panels 4 and 9) suggesting that in the zone of interest, deconvolution effectively attenuated the multiples. Note that the Spirit River multiple (between 0.65 and 1.0 s) has been significantly attenuated.

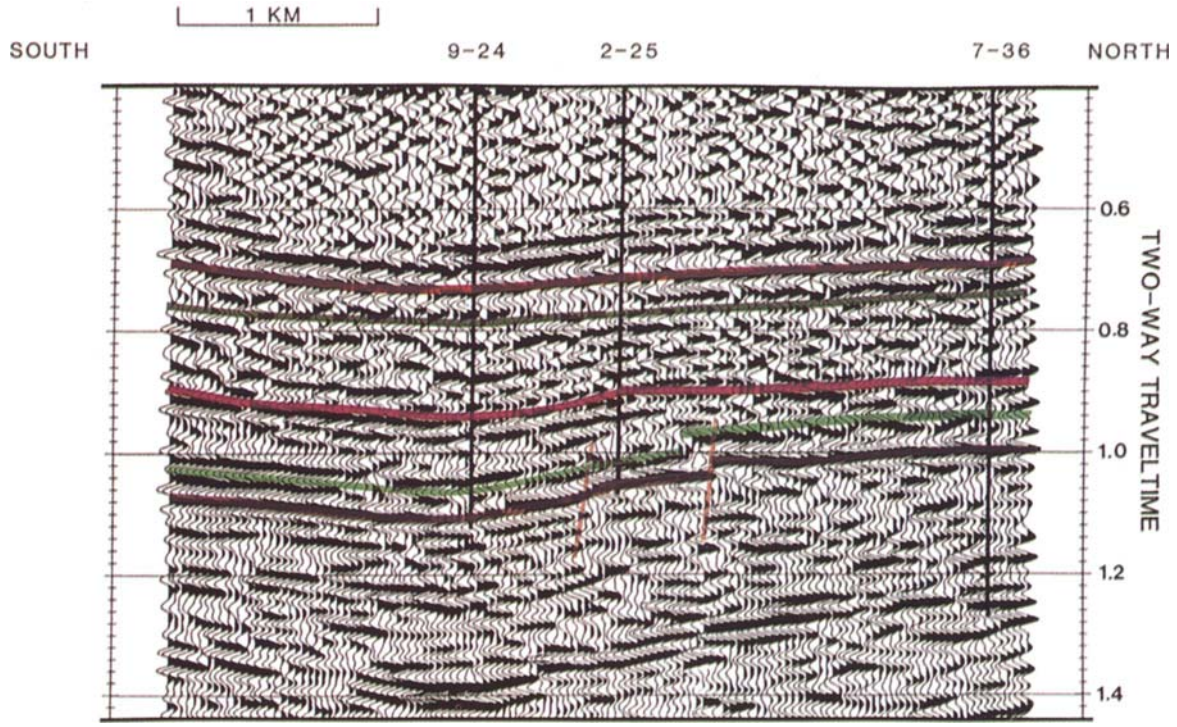

FIG. 4. Pre-VSP interpretation of the example surface seismic line. This north-south oriented line is situated about 200 m west of the 9-24 (VSP) well (Figure 3). (With increasing depth: orange-Nordegg; dark green-Halfway/Doig; purple-Belloy; light green-Basal Kiskatinaw; light brown-Debolt; brown-vertical faults).

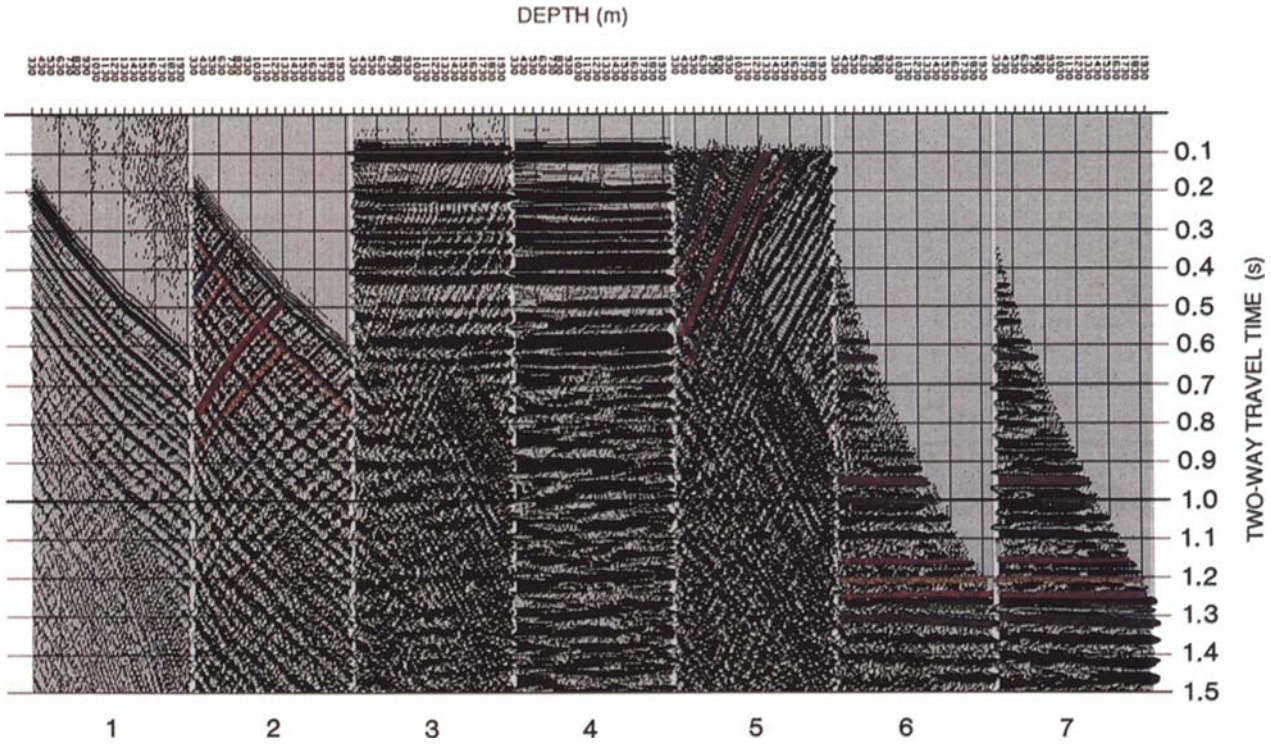

FIG. 5. Interpretive processing panel depicting the wavefield separation of the near-offset VSP. [1: raw field data (FRT); 2: gained raw data (FRT); 3: gained raw data (−TT); 4: separated downgoing waves (−TT); 5: separated upgoing waves (−TT); 6: upgoing waves (+TT); 7: median filtered upgoing waves (+TT)]. (Dark blue-Spirit River; orange-Nordegg; dark green-Halfway/Doig; purple-Belloy; yellow-Taylor Flats; red-Kiskatinaw; light green-Basal Kiskatinaw; light blue-Golata; light brown-Debolt).

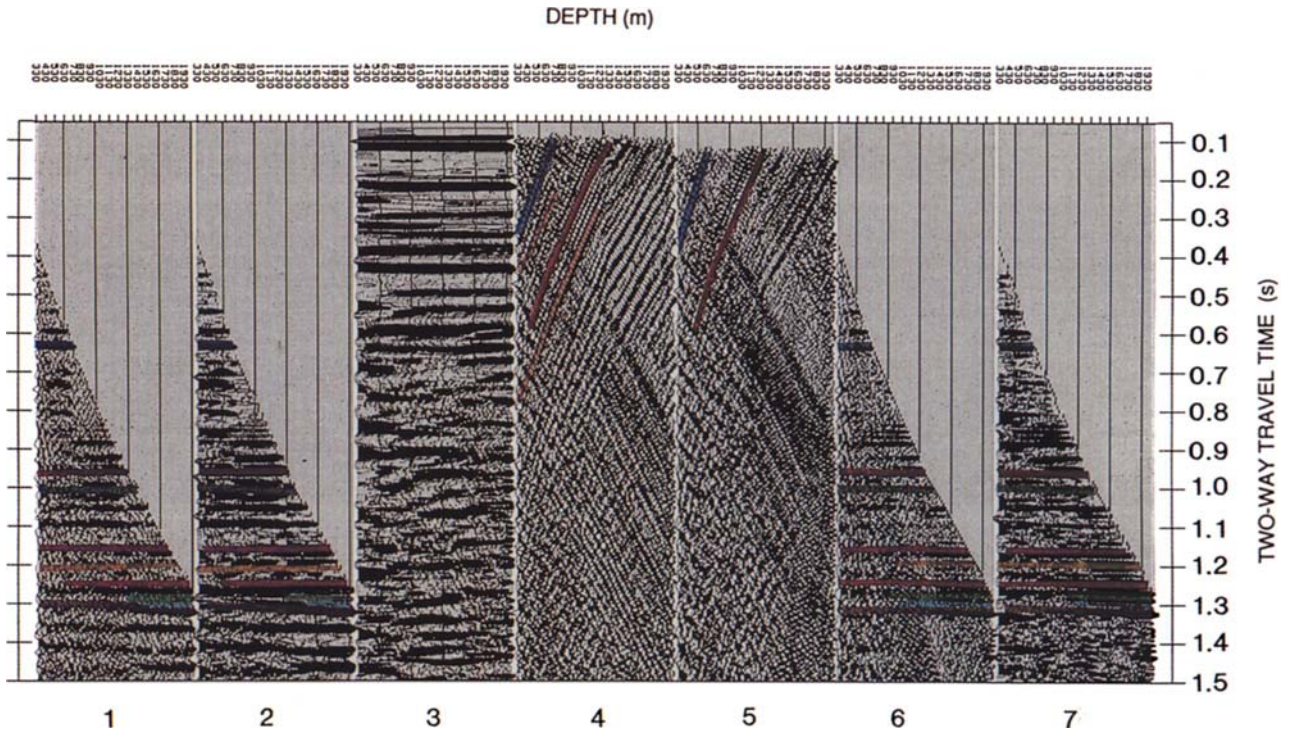

FIG. 6. Interpretive processing panel depicting the deconvolution of the near-offset VSP. [1: upgoing waves (+TT); 2: median filtered upgoing waves (+TT); 3: separated downgoing waves (−TT); 4: separated upgoing waves (−TT); 5: deconvolved, separated upgoing waves (−TT); 6: deconvolved, upgoing waves (+TT); 7: median filtered, deconvolved, upgoing waves (+TT)]. (Dark blue-Spirit River; orange-Nordegg; dark green-Halfway/Doig; purple-Belloy; yellow-Taylor Flats; red-Kiskatinaw; light green-Basal Kiskatinaw; light blue-Golata; light brown-Debolt).

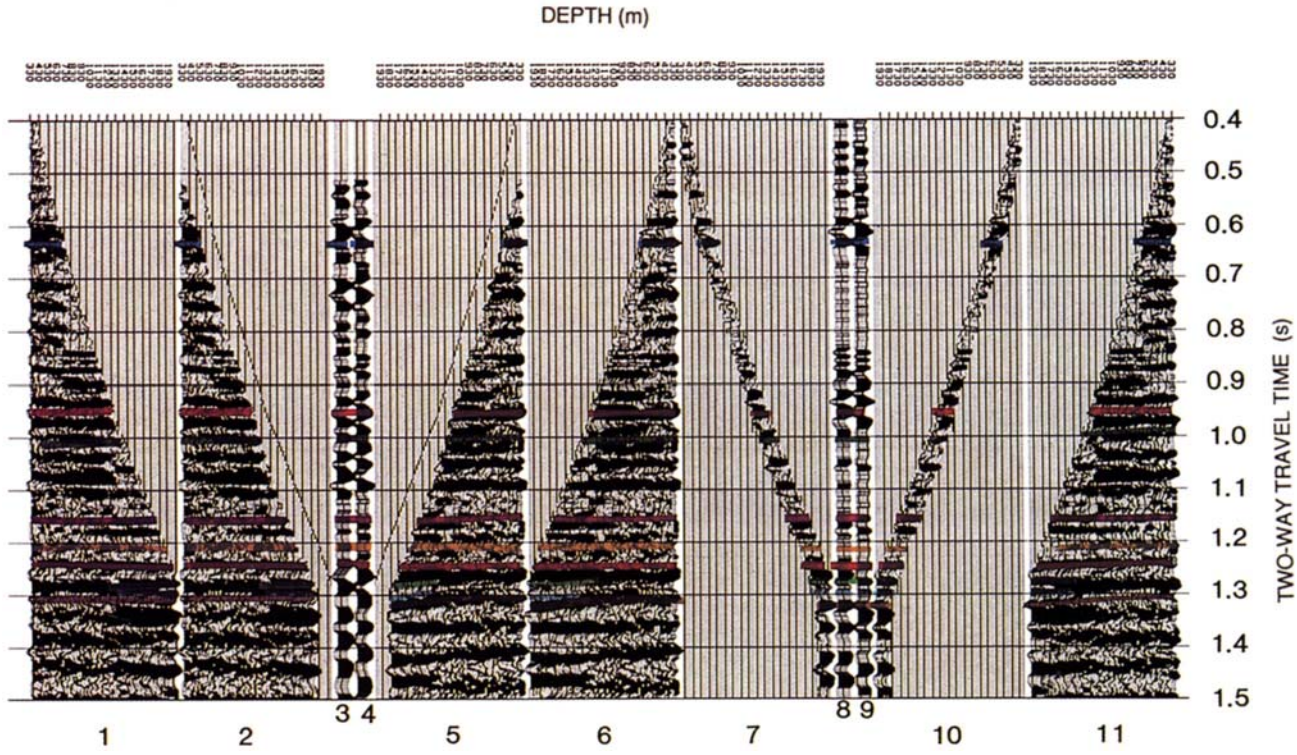

FIG. 7. Interpretive processing panel illustrating the use of nondeconvolved inside and outside corridor stacks. Panels 1, 2, 3, 9, 10, and 11 are reverse polarity. [1, 6, and 11: median filtered upgoing waves (+TT); 2 and 5: muted inside corridor (+TT); 3 and 4: inside corridor stacks (+TT); 7 and 10: muted outside corridor (+TT); 8 and 9: outside corridor stacks (+TT)]. (Dark blue-Spirit River; orange-Nordegg; dark green-Halfway/Doig; purple-Belloy; yellow-Taylor Flats; red-Kiskatinaw; light green-Basal Kiskatinaw; light blue-Golata; light brown-Debolt).

FAR-OFFSET VSP INTERPRETIVE PROCESSING: OFFSET LO1

On the far-offset LO1 VSP, the vertical (Z) and both horizontal (X and Y) axis data contain nonpartitioned elements of the upgoing and downgoing wavefields. Examination of the IPPs (Figures 9-11) reveals that the partitioning of the wavefields has significant implications with respect to interpretation. The LO1 IPPs are discussed and the following interpretive processing steps displayed below:

1) Hodogram-based rotation of the X, Y, and Z data (based on windowed data enveloping the *P*-wave first arrival; DiSiena et al., 1984);
2) Time-variant model-based rotations applied to the $HMAX_{up(derot)}$ and $Z_{up(derot)}$ data; and
3) The VSP-CDP transformation of the data (Dillon and Thomson, 1984).

Hodogram-based rotation; offset LO1

The raw X, Y, and Z data for the LO1 far-offset VSP are displayed in Figure 9 as panels 1, 2, and 3, respectively. The horizontal axis data (X and Y) are extremely noisy and contain only minor *P*-wave energy. The vertical axis data (Z) contains strong downgoing *P*-wave energy plus lower amplitude upgoing *P*-wave events. The hodogram-based rotation technique is designed to polarize these data so that the downgoing *P*-waves are presented on a single channel, HMAX′.

The first step illustrated in Figure 9, is the hodogram-based rotation of the X and Y data (corrects for phase changes because of tool rotation during the movement of the sonde up the borehole). The output HMIN and HMAX data are displayed as panels 4 and 5, respectively. HMIN and HMAX data are assumed to be aligned perpendicular and tangent to the plane formed by the source and wellbore, respectively. Note that HMIN [comprised of horizontally polarized shear (*SH*) wave events and out of the plane reflections], contains the dominant portion of the diffraction that appears at 1.0 s on the 650 to 800 m traces, suggesting that the diffraction is side-swipe energy originating from a fault feature out of the plane of the well and source.

The Z′ (panel 6) and HMAX′ (panel 7) data were obtained by rotating the Z and HMAX data using polarization angles estimated from a hodogram analysis in a window around the *P*-wave first arrival (DiSiena et al., 1984). This technique is designed to polarize the data so that the downgoing *P*-waves are effectively isolated on a single channel, HMAX′ (panel 7).

Time-variant model-based rotation: offset LO1

The time-variant, model-based polarization analysis interpretive processing panel is shown in Figure 10. The separated (using an f, k filter), upgoing waves from the Z′ and HMAX′ data are shown in panels 1 and 2 (Figure 10), respectively. These data are referred to as Z'_{up} and $HMAX'_{up}$. On both panels, upgoing *P*-waves from the Debolt, Golata, and Kiskatinaw can be interpreted, indicating that the hodogram-based rotations did not isolate the upgoing waves onto a single output panel.

To remove the effects of the Z to Z′, and HMAX to HMAX′ transformations (necessary to isolate the downgoing *P*-waves), the Z'_{up} and $HMAX'_{up}$ were derotated (using the inverse operation of the second polarization rotation). The output data of the derotation process, namely the $Z_{up(derot)}$ and $HMAX_{up(derot)}$, are shown as panels 3 and 4 of Figure 10, respectively. The upgoing *P*-wave events have been effectively distributed back onto the Z-type axis, $Z_{up(derot)}$. Unlike the upgoing wave events in the raw Z data (panel 3 in Figure 9), where the downgoing *P*-waves were predominant, the separated upgoing *P*-wave events in the $Z_{up(derot)}$ data are dominant and interpretable.

On the $Z_{up(derot)}$ data (panel 3), upgoing *P*-waves generated by shallow reflectors (such as the Spirit River) are improperly aligned (because of the choice of rotation angles). These data have been derotated, but the upgoing *P*-wave events are still partitioned on both output data ($Z_{up(derot)}$ and $HMAX_{up(derot)}$ because of the nonzero offset of the source. The deeper events do not suffer much misalignment because deep event raypath geometries satisfy the near-vertical incidence angle assumption better than the raypaths of shallower events. The time-variant model-based rotation corrects for this misalignment. The output upgoing wave displays, $HMAX''_{up}$ and Z''_{up}, are shown on panels 5 and 6, respectively. Note that the shallow events display more alignment than on the $Z_{up(derot)}$ (panel 3). The rotation angle required for the Spirit River and Nordegg event on a particular trace was different from the rotation angle for deeper events (such as the Debolt) on the same trace. The time-variant rotation technique generated these different rotation angles.

The Spirit River event is barely discernable on the Z''_{up} data because the reflected raypaths for this shallow event are at or near the critical angle. The surface-generated multiples from the Spirit River interface (observed on the nondeconvolved near-offset data of panel 7 in Figure 5) are significantly lower in amplitude on the far-offset data (panel 6; Figure 10).

VSP-CDP transformation: offset LO1

Nonmedian and median filtered versions of the Z''_{up} data are displayed (pseudo two-way traveltime versus depth) in Figure 11 as panels 1 and 2, respectively. The VSP-CDP transformed (pseudo two-way traveltime versus offset) data are shown as panel 3. Reverse-polarity displays of these data are presented as panels 6, 5, and 4, respectively.

The LO1 source was 700 m from 9-24 and in the direction of well 2-25 (more-or-less paralleling the surface seismic line). The interpretation of the surface seismic data (Figure 3) suggests that a major Debolt fault was located between these two wells. The LO1 data support this thesis. More specifically, on panel 3 (Figure 11), the Debolt is interpreted to be faulted between these wells. A second interesting feature on panel 3 is that the signature of the basal Kiskatinaw event changes abruptly in proximity to the fault nearest 9-24. The basal Kiskatinaw event, as interpreted, is continuous at greater offsets, but is substantially decreased in amplitude. This character change could indicate a change in lithology or porosity.

The upper Kiskatinaw (hydrocarbon reservoir at 9-24), as interpreted on panel 3, is laterally continuous but faulted.

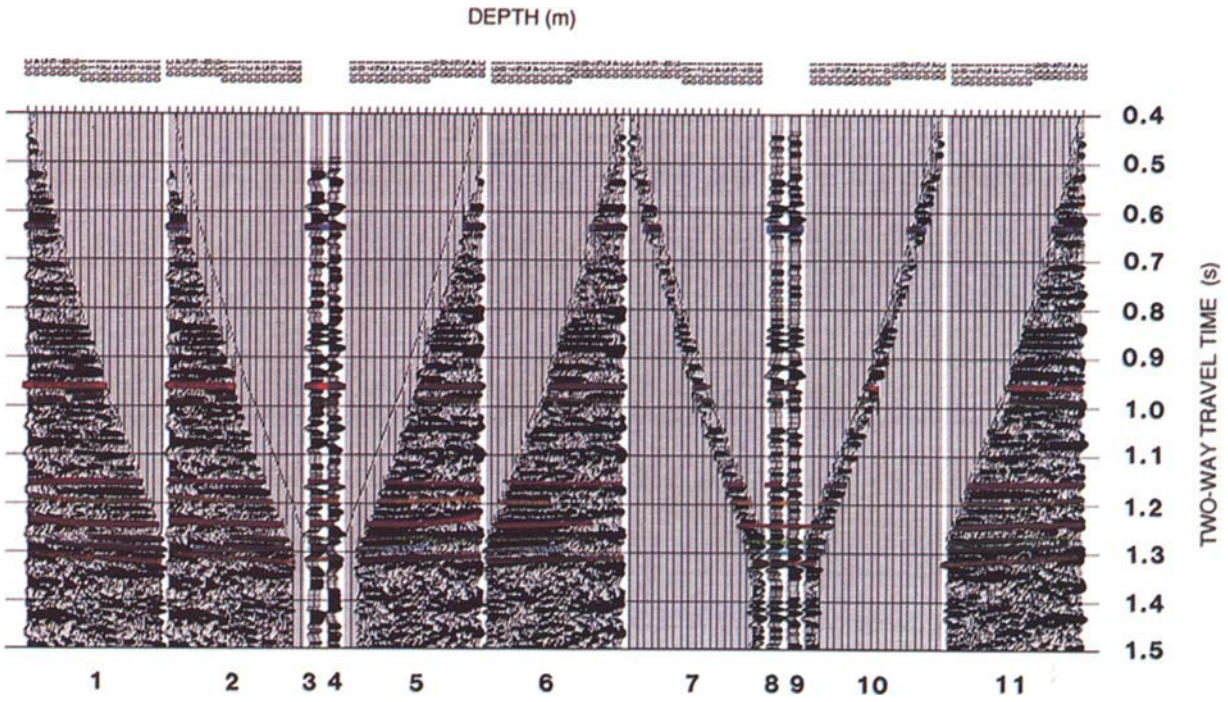

FIG. 8. Interpretive processing panel illustrating the use of deconvolved inside and outside corridor stacks. Panels 1, 2, 3, 9, 10, 11 are reverse polarity. [1, 6 and 11: median filtered upgoing waves (+TT); 2 and 5: muted inside corridor (+TT); 3 and 4: inside corridor stacks (+TT); 7 and 10: muted outside corridor (+TT); 8 and 9: outside corridor stacks (+TT)]. (Dark blue-Spirit River; orange-Nordegg; dark green-Halfway/Doig; purple-Belloy; yellow-Taylor Flats; red-Kiskatinaw; light green-Basal Kiskatinaw; light blue-Golata; light brown-Debolt).

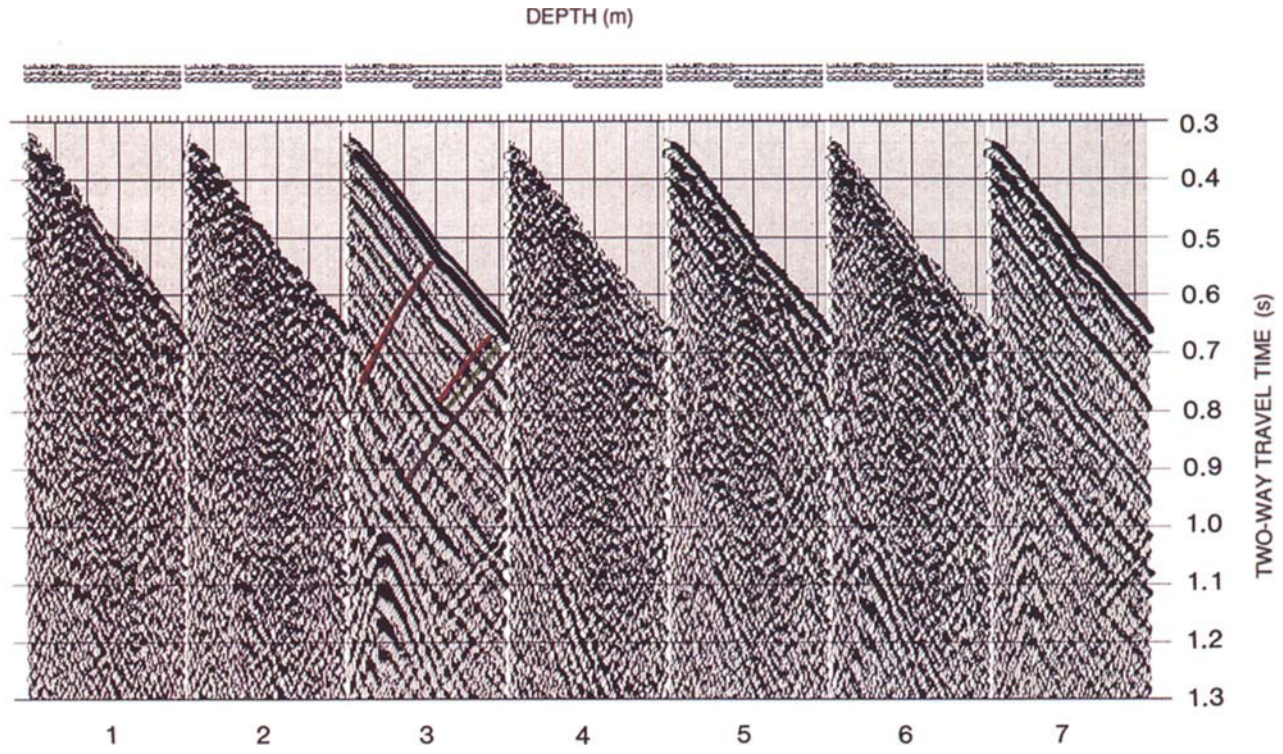

FIG. 9. Interpretive processing panel depicting the hodogram-based rotation of the LO1 far-offset VSP. [1: X-axis (FRT); 2: Y-axis (FRT); 3: Z-axis (FRT); 4: HMIN (FRT); 5: HMAX (FRT); 6: Z′-axis (−TT); 7: HMAX′ (FRT)]. (Dark blue-Spirit River; orange-Nordegg; dark green-Halfway/Doig; purple-Belloy; yellow-Taylor Flats; red-Kiskatinaw; light green-Basal Kiskatinaw; light blue-Golata; light brown-Debolt).

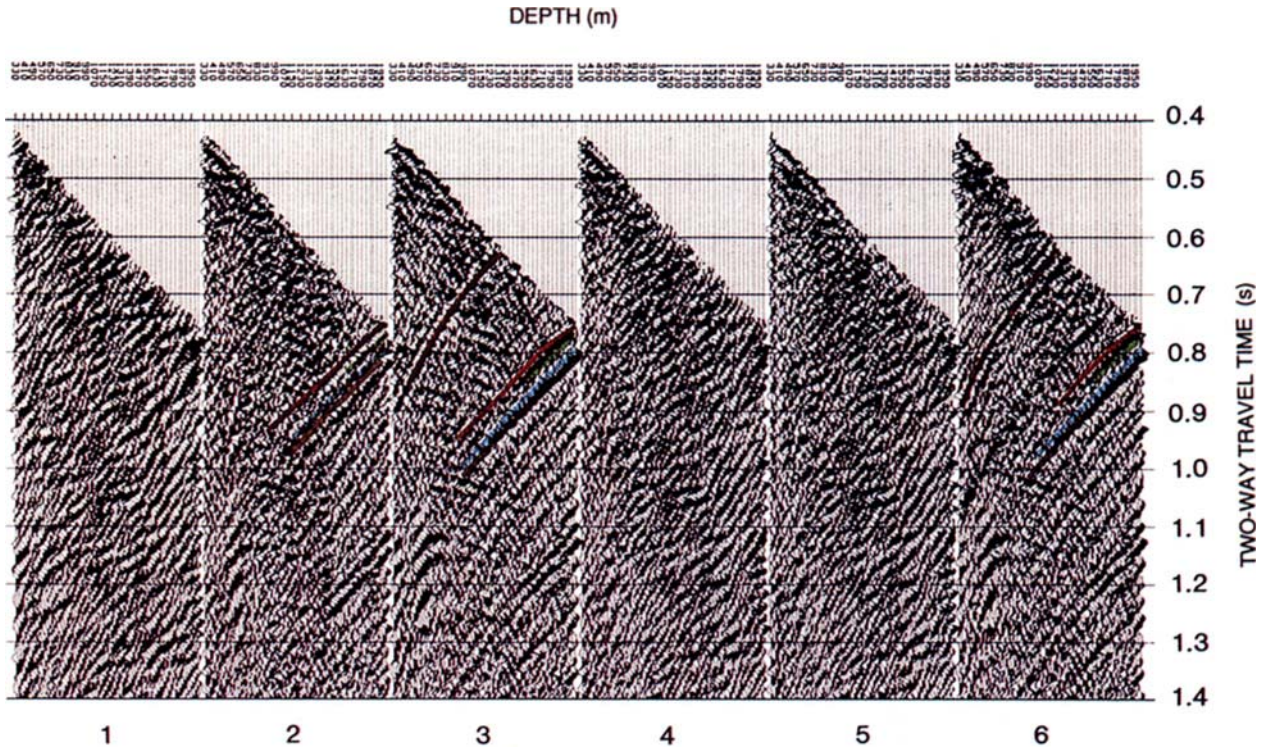

FIG. 10. Interpretive processing panel depicting the time-variant model-based rotation of the LO1 far-offset VSP. [1: Z'_{up} (FRT); 2: $HMAX'_{up}$ (FRT); 3: $Z'_{up(derot)}$ (FRT); 4: $HMAX_{up(derot)}$ (FRT); 5: $HMAX''_{up}$ (FRT); 6: Z''_{up} (FRT)]. (Dark blue-Spirit River; orange-Nordegg; dark green-Halfway/Doig; purple-Belloy; yellow-Taylor Flats; red-Kiskatinaw; light green-Basal Kiskatinaw; light blue-Golata; light brown-Debolt).

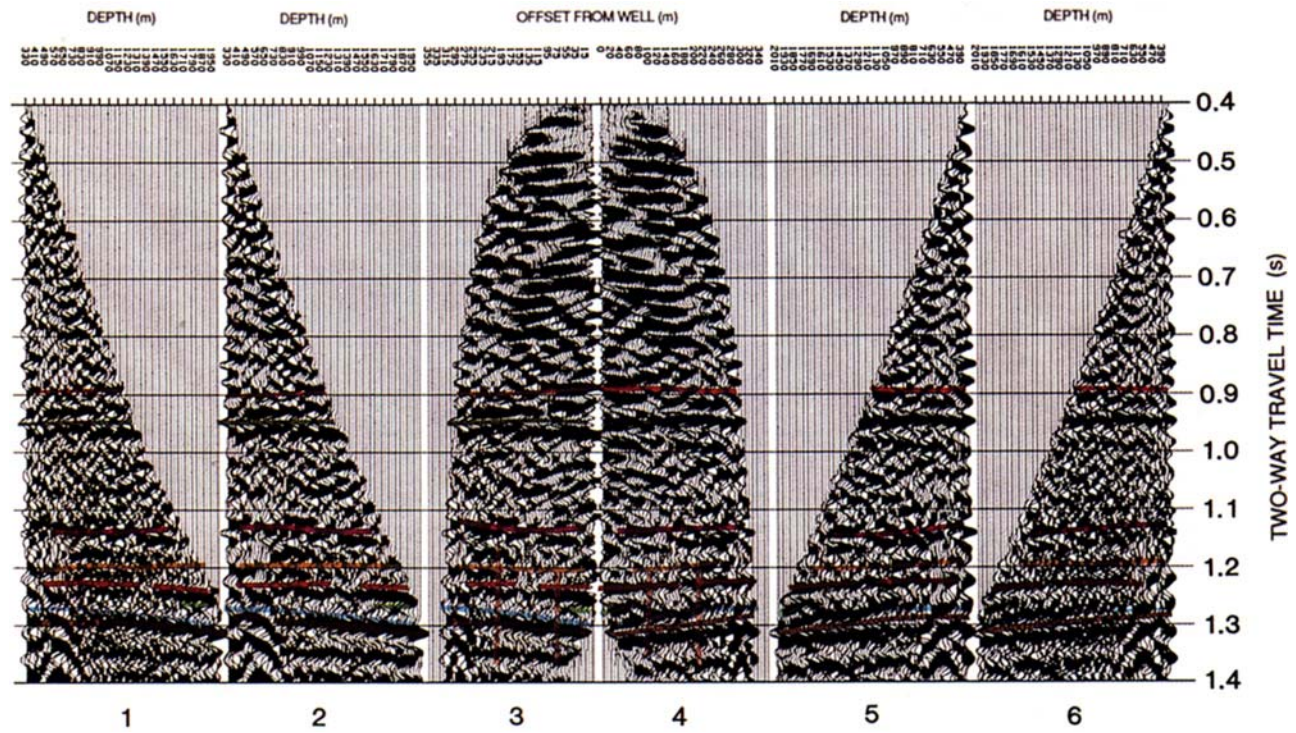

FIG. 11. Interpretive processing panel showing the VSP-CDP transformation of the LO1 far-offset VSP. Panels 4, 5, and 6 are reverse polarity. [1 and 6: Z'_{up} (FRT); 2 and 5: median filtered Z''_{up} (FRT); 3 and 4: median filtered Z''_{up} VSP-CDP (FRT)]. (Dark blue-Spirit River; orange-Nordegg; dark green-Halfway/Doig; purple-Belloy; yellow-Taylor Flats; red-Kiskatinaw; light green-Basal Kiskatinaw; light blue-Golata; light brown-Debolt; brown-vertical faults).

Vertical displacement is interpreted across two faults. This thesis is supported by well control; the upper Kiskatinaw is present in both 9-24 and 2-25. At 9-24 the upper Kiskatinaw forms a gas reservoir; in the structurally higher 2-25 well, this unit is nonproductive.

FAR-OFFSET VSP INTERPRETIVE PROCESSING: OFFSET LO2

The LO1 far-offset source was 741 m east of 9-24. These data were acquired to map the lateral extent of the upper Kiskatinaw reservoir to the east of 9-24, and to provide a higher resolution seismic image of Debolt faults. The recording and processing of these data was similar to that described for the LO1 survey.

In the first stage of interpretive processing, a hodogram-based rotation technique polarized the X, Y, and Z data, so that the downgoing *P*-waves were presented on a single channel, HMAX′. The filtered output data, Z'_{up} and $HMAX'_{up}$, were derotated and time-variant model-based rotations were applied to the output data. In the final stage, the Z''_{up} data were displayed in pseudo transit time versus depth, and in pseudo transit time versus offset.

The Z''_{up} data after the application of the VSP-CDP transform is displayed in Figure 12. Nonmedian and median filtered versions of the Z''_{up} data are displayed (pseudo two-way traveltime versus depth) as panels 6 and 5, respectively. The VSP-CDP transformed (pseudo two-way traveltime versus offset) data are shown as panel 4. Reverse-polarity displays of these data are presented as panels 1, 2, and 3, respectively.

The data in panel 4 image 2 faults, both of which are of the same magnitude as those on the LO1 data (Figure 11). The basal Kiskatinaw event is interpreted to exhibit a laterally continuous seismic signature. This is unlike the character of the basal Kiskatinaw which decreases in amplitude beyond the first imaged fault. The upper Kiskatinaw (hydrocarbon reservoir at 9-24), as interpreted on panel 4, is laterally continuous but faulted.

INTEGRATED INTERPRETATION

On the left-hand side of the integrated interpretative display (Figure 13), gamma ray logs for the 9-24, 2-25, and 7-36 wells are time-tied to the post-VSP interpretation of surface seismic data. On the right-hand side, near-offset VSP data are time-tied to the 9-24 gamma ray and sonic logs. These correlated data allow for the confident interpretation of the surface seismic line and the identification of the Spirit River, Nordegg, Halfway/Doig, Belloy, Taylor Flat, upper Kiskatinaw, basal Kiskatinaw, Golata, and Debolt. The nondeconvolved version of the VSP data is presented to facilitate the analysis of multiple contamination. As evidenced by a comparison of the surface seismic line and the corridor stacks, the multiple-contaminated inside corridor stack provides a poor tie to the data at the zone of interest

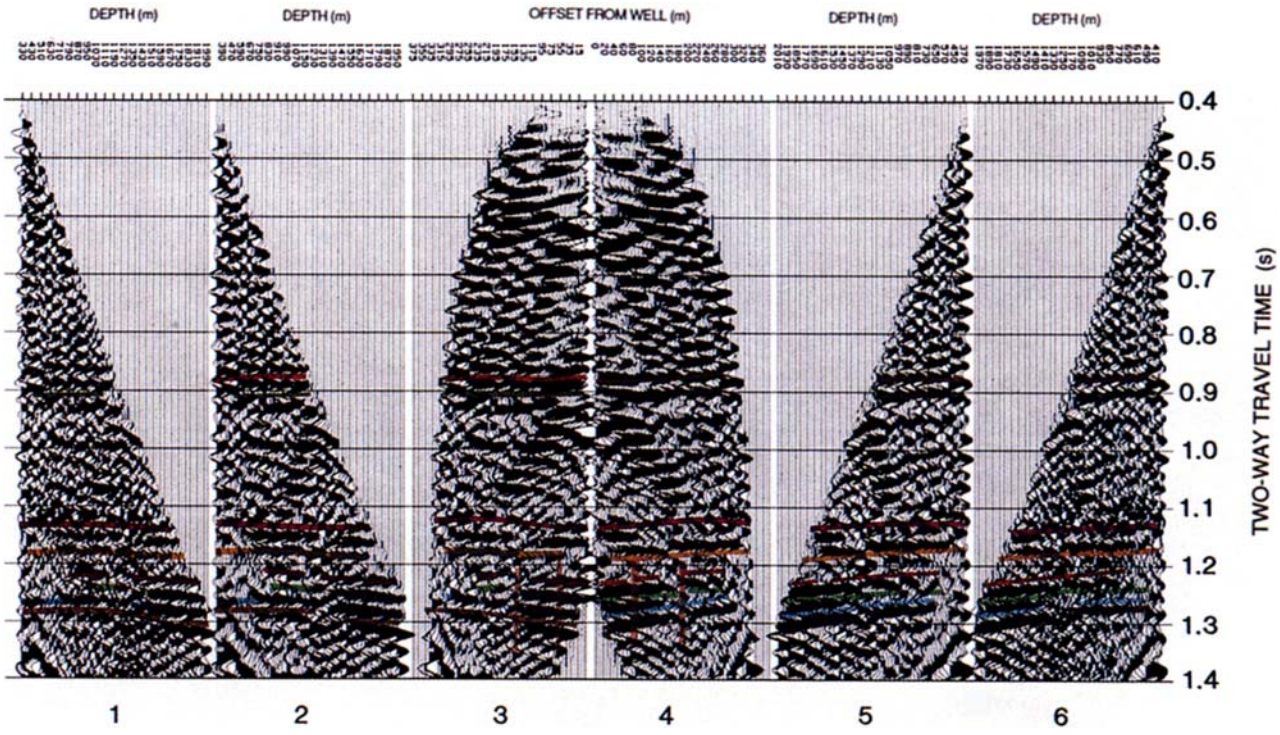

FIG. 12. Interpretive processing panel showing the VSP-CDP transformation of the LO2 far-offset VSP. Panels 2, 4, and 5 are reverse polarity. [1 and 6: Z'_{up} (FRT); 2 and 5: median filtered Z'_{up} (FRT); 3 and 4: median filtered Z''_{up} VSP-CDP (FRT)]. (Dark blue-Spirit River; orange-Nordegg; dark green-Halfway/Doig; purple-Belloy; yellow-Taylor Flats; red-Kiskatinaw; light green-Basal Kiskatinaw; light blue-Golata; light brown-Debolt).

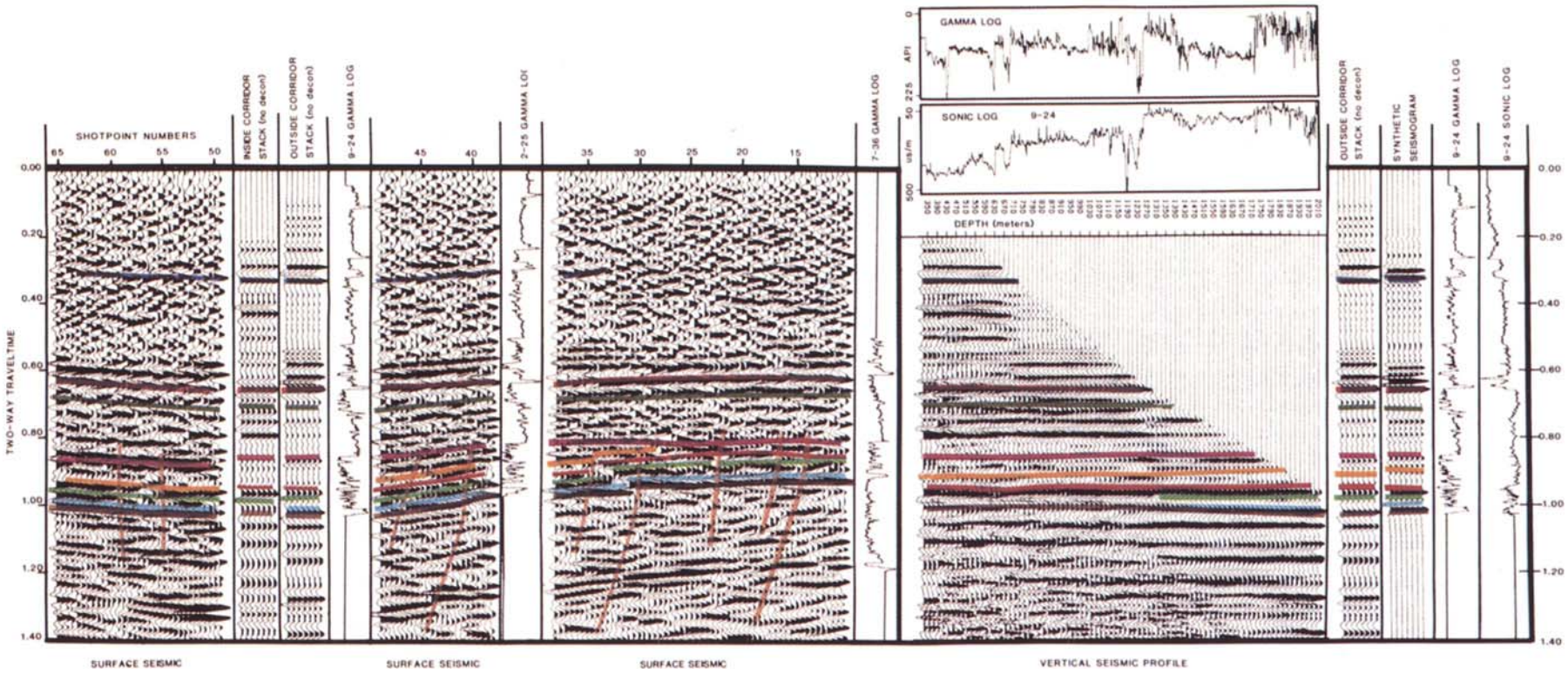

FIG. 13. Integrated interpretive display (IID) showing the interpretation of the available exploration data. (Dark blue-Spirit River; orange-Nordegg; dark green-Halfway/Doig; purple-Belloy; yellow-Taylor Flats; red-Kiskatinaw; light green-Basal Kiskatinaw; light blue-Golata; light brown-Debolt; brown-vertical faults).

(Kiskatinaw). This suggests that multiples on the surface seismic data have been effectively attenuated.

The post-VSP version of the surface seismic section (normal polarity display; Figure 14) differs slightly from the pre-well interpretation (Figure 4) in several respects. Of particular significance is that on the updated version, the Taylor Flat and Kiskatinaw events are confidently correlated. Note that in the post-VSP interpretation, the Taylor Flat event is absent at 7-36. This interpretation is supported by the well log control. On the basis of the post-VSP interpretation of the surface seismic line and the analysis of the far-offset VSP data, the geologic cross-section of Figure 15 was constructed. This geologic section is consistent with the well log, surface seismic, and seismic profile control.

CONCLUSIONS

On the basis of conventional surface seismic data, the exploratory 9-24 well was drilled on the downthrown side of a fault block. The expectation was that the gas-prone sandstones of the basal Kiskatinaw would be laterally truncated and sealed against the upthrown fault. Contrary to expectations, the basal Kiskatinaw was unproductive; however, 9-24 did encounter commercial gas within the upper Kiskatinaw and is now shut-in.

To obtain a high-resolution seismic image of the subsurface in the vicinity of 9-24, and to evaluate the proximity of any fault features that might not have been resolved on the surface seismic data, three VSP surveys were run. This seismic profiling information, in conjunction with surface seismic coverage, was used to image the subsurface fault pattern, and elucidate the seismic signature and lateral continuity of the upper Kiskatinaw. The profile data supplemented the surface seismic and well log control in that:

1) VSP data could be directly correlated to the surface seismic. As a result, the surface seismic control could be accurately tied to the subsurface geology;
2) Multiples could be identified on the VSP data and subsequently deconvolved out of the surface seismic data; and
3) The subsurface, in the vicinity of the borehole, was better resolved on the VSP data than on the surface seismic control.

The information provided by the VSP surveys allowed the geophysicists to refine their interpretation of the surface seismic data and enabled the construction of a detailed geologic cross-section. These interpretations provide information with respect to the subsurface in proximity to 9-24, and perhaps more importantly, further elucidate the geologic history of the structurally complex Fort St. John Graben area.

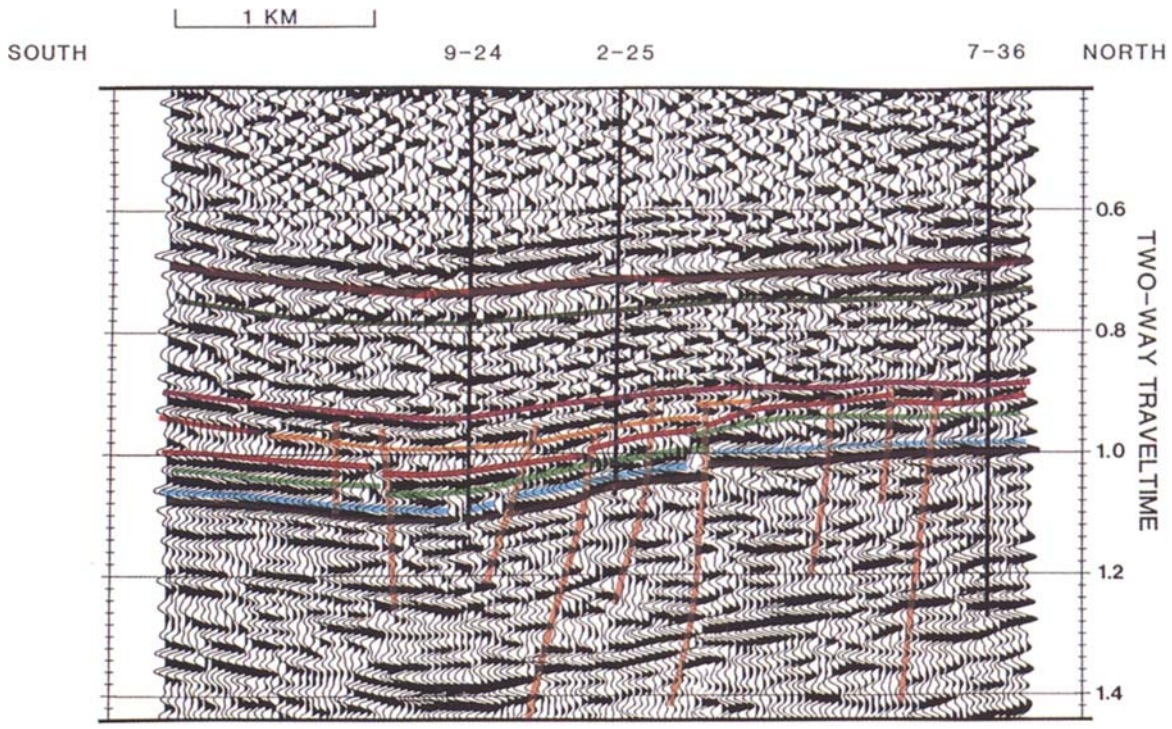

FIG. 14. Post-VSP interpretation of the example surface seismic line (Figure 4). (Dark blue-Spirit River; orange-Nordegg; dark green-Halfway/Doig; purple-Belloy; yellow-Taylor Flats; red-Kiskatinaw; light green-Basal Kiskatinaw; light blue-Golata; light brown-Debolt; brown-vertical faults).

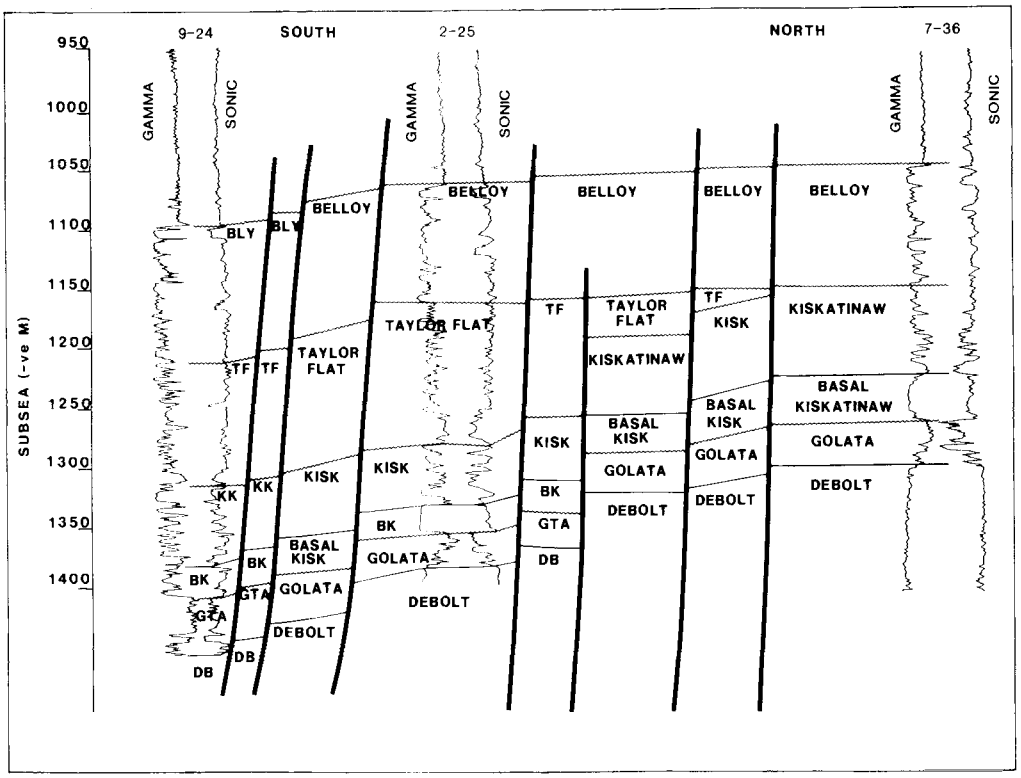

FIG. 15. Geologic cross-section incorporating 9-24, 2-25, and 7-36 well log. The interwell interpretation is constrained by the surface seismic and VSP data.

ACKNOWLEDGMENTS

BP Resources Canada Ltd. generously authorized the publication of the proprietary seismic data. Computalog Ltd. of Calgary provided access to the Halliburton Geophysical Inc. VSP processing system. BP Resources Canada Ltd., Inverse Theory and Application Inc., Anglo-American Prospecting Services, and the University of Pretoria allowed us to use their respective seismic data processing systems. Partial support was provided by the National Geophysics Program of South Africa. Our thanks are extended to Professor P. G. (Pat) Eriksson; his constructive criticisms were appreciated.

REFERENCES

Barclay, J. E., 1988, The Lower Carboniferous Golata Formation of the Western Canada Basin the context of sequence stratigraphy, *in* James, D. P., and Leckie, D. A., Eds., Sequences, stratigraphy, sedimentology: Surface and subsurface: Can. Soc. Petr. Geol., Memoir **15**, 1–14.

Dillon, P. B., and Thomson, R. C., 1984, Offset source VSP surveys and their image reconstruction: Geophys. Prosp., **32**, 790–811.

DiSiena, J. P., Gaiser, J. E., and Corrigan, D., 1984, Horizontal components and shear wave analysis of three-component VSP data, *in* Toksöz, N. M., and Stewart, R. R., Eds., Vertical seismic profiling: Advanced concepts: Geophys. Press, 177–188.

Gazdag, J., 1978, Wave-equation migration by phase shift: Geophys., **43**, 1342–1351.

Gazdag, J., and Squazzero, P., 1984, Migration of seismic data by phase shift plus interpolation: Geophys., **49**, 129–131.

Hale, I. D., 1984, Dip-moveout by Fourier transform: Geophys., **49**, 741–757.

Hardage, B. A., 1985, Vertical seismic profiling: Geophys. Press, 2nd ed.

Hinds, R. C., Kuzmiski, R. K., Botha, W. J., and Anderson, N. L., 1989, Vertical and lateral seismic profiles, *in* Anderson, N. L., Hills, L. V., and Cederwall, D. A., Eds., Geophysical atlas of western Canadian hydrocarbon pools: Can. Soc. Expl. Geophys./ Can. Soc. Petr. Geol., 319–344.

Richards, B. C., 1989, Upper Kaskaskia sequence, uppermost Devonian and Lower Carboniferous, *in* Ricketts, B. D., Ed., The Western Canadian Sedimentary Basin, a case history Can. Soc. Petr. Geol., 165–201.

——— 1990, Tectonic and depositional history of the Early Carboniferous Peace River Embayment, Alberta and British Columbia, *in* Basin Perspectives: Can. Soc. Petr. Geol., Program and Abstracts, 118.

Richards, B. C. Bamber, E. W., Higgins, A. C., and Utting, J., Carboniferous, *in* Scott, D. F., and Aitken, J. D., Eds., Sedimentary cover of the craton: Canada, (Stratigraphy): Geol. Surv. Can., in press.